PERGAMON

Journal of Geodynamics 33 (2002) 131–142

JOURNAL OF
GEODYNAMICS

www.elsevier.com/locate/jgeodyn

Gradients in the interpretation of satellite-altitude magnetic data: an example from central Africa

D. Ravat[a,*], B. Wang[a], E. Wildermuth[a], Patrick T. Taylor[b]

[a]*Department of Geology MS 4324, Southern Illinois University Carbondale, Carbondale, IL 62901-4324, USA*
[b]*Geodynamics Branch Code 921, NASA/GSFC, Greenbelt, MD 20771, USA*

Abstract

The Euler and the analytic signal methods have been implemented in spherical coordinates to facilitate the interpretation of spherically-registered potential-field anomaly data collected by satellites. Model studies show that the methods are able to delineate the edges of idealized models even from 400 km altitude; the depth resolution is, however, not adequate from this altitude. A very large magnetic anomaly, the Bangui anomaly in central Africa, was studied using these methods. These results, from Magsat data, suggest that impact related remagnetization (Girdler, R.W.,Taylor, P.T., Frawley, J.J., 1992, A possible impact origin for the Bangui magnetic anomaly (Central Africa), Tectonophysics, 212, 45–58) and presence of a highly magnetic source (Ravat, D., Hinze, W.J., von Frese, R.R.B., 1992, Analysis of Magsat magnetic contrasts across Africa and South America. Tectonophysics 212, 59–76) near the center of the impact structure are likely contributors to the anomaly.

1. Introduction

Gradient methods have been extremely useful in the interpretation of near-surface potential-field anomalies because they increase the resolution of the edges of geologic sources and de-emphasize the effect of the background or 'regional' field. Two methods based on the anomaly gradients, Euler (Thompson, 1982; Reid et al., 1990) and the analytic signal (Nabighian, 1972, 1974; Roest et al., 1992) have proven particularly effective in the semi-automatic interpretation of magnetic anomaly data (i.e. determination of source outline and depths of sources). The methods are objective and not affected by the geometry of changing magnetic field directions or remanent

* Corresponding author. Tel.: +1-618-453-7352; fax: +1-618-453-7393.
E-mail address: ravat@geo.siu.edu (D. Ravat).

0264-3707/02/$ - see front matter
PII: S0264-3707(01)00059-X

magnetization of the sources. So far, the gradient-based interpretation methods have not been applied in the interpretation of the satellite-altitude magnetic anomaly data.

Satellite-altitude magnetic measurements have generally been collected at altitudes exceeding 300 km (e.g. POGO, Magsat, Oersted, and CHAMP). At these high altitudes, magnetic fields from the sources in the Earth's lithosphere are relatively small (<30 nT) with long-wavelengths (>400 km), and effects from many geologic sources merge to form the observed anomalies. Thus, gradient-based methods may improve the resolution of regional variations of magnetizations producing these satellite data and their geologic interpretation. In general, however, noise is also present in the derived anomalies from various sources such as the measurement uncertainty and the removal of the main and the external fields and, unfortunately, the computation of gradients also enhances the noise. Thus, the smaller signal-to-noise ratio of the satellite-altitude magnetic anomalies, in comparison to the near surface magnetic observations, could render the results of such methods unusable. In this study, we examine the utility of these techniques to the interpretation of satellite altitude magnetic data using idealized geometric models. We then apply these techniques to the Bangui (Central African Republic) magnetic anomaly in central Africa.

A magnetic anomaly map prepared from POGO data first showed the full extent of the Bangui magnetic anomaly (Regan et al., 1975). The anomaly is dipolar (i.e. near the magnetic equator, an inductively magnetized source produces a magnetic low with two positive side lobes to the north

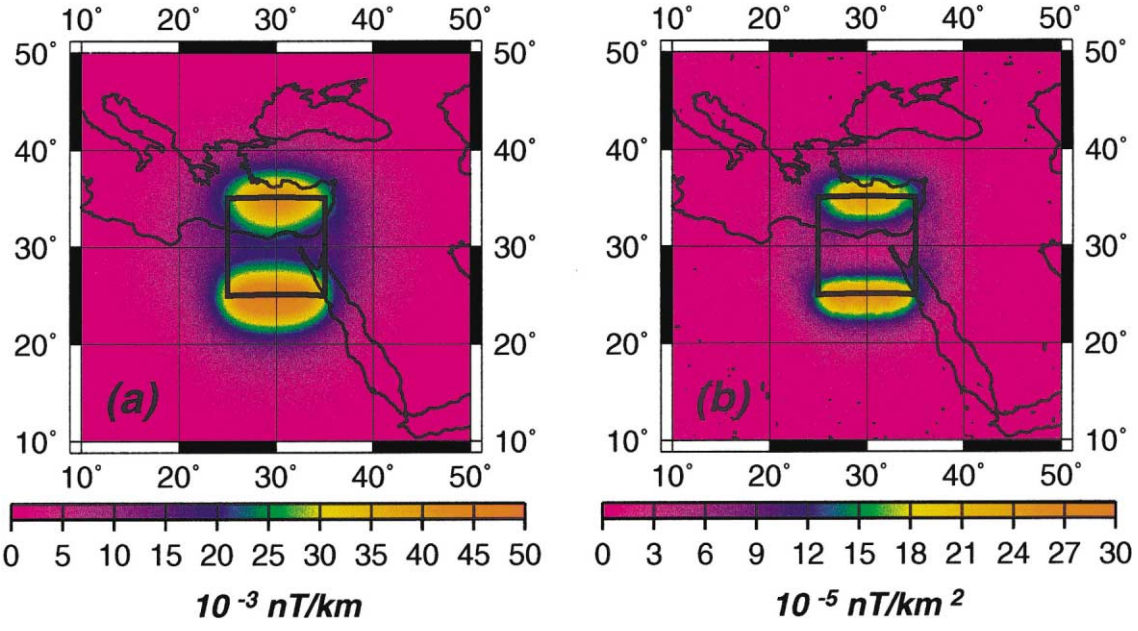

Fig. 1. The amplitude of the analytic signal of (a) the total intensity magnetic anomaly, and (b) the first vertical derivative of the anomaly from a prismatic source. The units of the amplitude of the analytic signal are of the derivative of the field from which it was computed; they are displayed on the figure. The outline of the induced prismatic source (40 km thick at the Earth's surface) is shown by the heavy lines; however, the method is not affected by the direction of the geomagnetic field or the presence of remanence. The amplitude of the analytic signal being an absolute quantity, the color scale consists of only positive numbers. Observation elevation = 400 km. Grid spacing = 0.5°.

and south) and has been the subject of different interpretations. Green (1976) suggested that the source was extensive, deep, and highly magnetic, speculating that it could be a massive iron meteorite. Regan and Marsh (1982) proposed as the source a highly magnetic intrusive body under the Oubangui basin in central Africa. Hastings (1982), however, interpreted it as a region of magnetized Precambrian shield flanked on the north and the south by the Chad and the Congo basins, respectively. Ravat (1989) and Ravat et al. (1992) considered the geologic contributions of sources in central Africa (such as the Angola, Kasai, and Central African shields, the Chad and the Congo Basin, and the Central African rift). An additional increase in magnetization was, however, required to account for this anomaly, which was attributed to meteoritic material (e.g. Green, 1976). Girdler et al. (1992) suggested an impact related origin for the anomaly. Evidence for this was based on an apparent double-ring structure observed in the East-gradient of the 5-min topographic data as well as the magnetic and gravity anomaly fields (see Fig. 2 in Girdler et al., 1992). They modeled the source of the anomaly with an 800 km diameter thin circular disc possessing both induced and remanent magnetization and situated directly beneath the topographic ring. This latter interpretation has been controversial because very ancient age (Early Precambrian or earlier) has been inferred by Girdler et al. (1992) for this large diameter impact (based apparently on the frequency of impacts of various size on terrestrial planets and the Moon, Grieve, 1987) and yet the ring structure (if the topographic ring itself is not an illusion) appears to have survived through the processes of erosion and crustal deformations during the late Precambrian and Mesozoic times. If the Bangui impact is indeed ancient, then the present

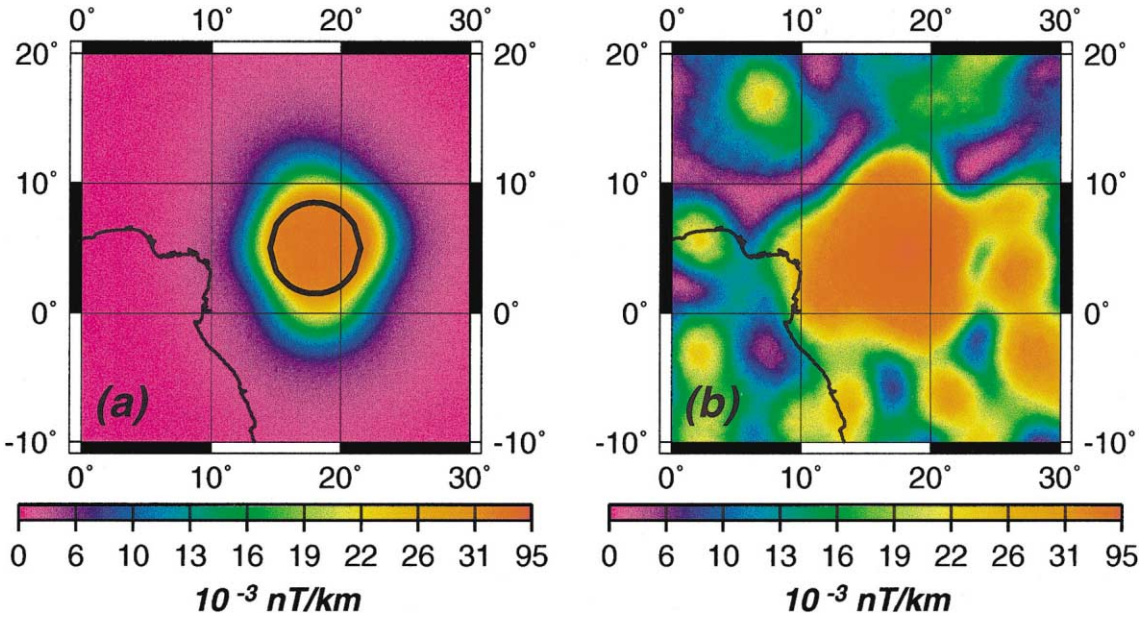

Fig. 2. The amplitude of the analytic signal of the total intensity magnetic anomaly from (a) the impact model of Girdler et al. (1992) for the Bangui anomaly in central Africa, and (b) the anomaly field of Cain et al. (1990) for the central African region. The heavy line shows the outline of the impact model. Observation elevation = 400 km. Grid spacing = 0.5°. See the caption of Fig. 1 for the details regarding the units and color scale.

observed topographic rings may, however, be a scar or the relict of the impact's rings. Because both the gradient methods we are developing are objective, they are used here in an effort to discriminate between these competing models of the origin of the Bangui magnetic anomaly.

Instead of the total field anomalies, the methods discussed here could also be used on the vector components. For the Magsat data used in this paper, the vector components are affected by noise originating from the uncertainty in attitude determination—the scalar field is not. The effect of this noise in the Magsat vector data will be significantly enhanced by taking higher order derivatives and, therefore, we did not use the vector anomalies in this study.

1.1. The analytic signal method

Analytic signal is formed by combining derivatives of the potential field (Blakely, 1995). The amplitude of the analytic signal has desirable properties for the interpretation of magnetic anomalies (Nabighian, 1972, 1974; Roest et al., 1992); specifically, the maxima of this function overlie the source edges and are related to the source depth. The generalized amplitude of the analytic signal, $|A_n|$, which is computed from the derivatives of the field in the *local magnetic coordinate system*, is defined by Hsu et al. (1996,1998) as

$$|A_n| = \sqrt{\left[\frac{\partial}{\partial x}\left(\frac{\partial^n T}{\partial z^n}\right)\right]^2 + \left[\frac{\partial}{\partial y}\left(\frac{\partial^n T}{\partial z^n}\right)\right]^2 + \left[\frac{\partial}{\partial z}\left(\frac{\partial^n T}{\partial z^n}\right)\right]^2}, \tag{1}$$

where T is the total intensity magnetic anomaly and n is the order of the derivative. Instead of the derivative $\frac{\partial^n T}{\partial z^n}$, one could theoretically take a derivative in any direction, but from the perspective of analyzing geologic sources it is sensible to consider the vertical variation of the anomaly field, T. Also, the situation $n=0$ implies the use of the method directly on the anomaly field (the notation is algebraically valid, as $\frac{\partial^0}{\partial z^0}=1$). For satellite-altitude magnetic data, where the anomalies are mapped as a function of latitude (θ) and longitude (ϕ), the gradients are first converted to the local magnetic coordinate system (x, y, and z pointing to Geographic North, East, and down directions, respectively) using relations, $\frac{\partial}{\partial x}=\frac{1}{r}\frac{\partial}{\partial \theta}$ and $\frac{\partial}{\partial y}=\frac{1}{r\ \sin\ \theta}\frac{\partial}{\partial \phi}$, respectively, where r is the distance from the Earth's center to the observation altitude. The z-derivatives $\left(\frac{\partial}{\partial z}\right)$ are computed using the difference between the anomaly fields 10 km apart in elevation, since the field changes very slowly at 400 km altitude (the value of $\sim$10 km of vertical difference in elevation to obtain meaningful vertical derivatives at 400 km altitude was arrived at through experimentation by Ravat (1989) for his first and second vertical derivative calculations). This altitude is approximately the average elevation of the global Magsat data (Langel and Hinze, 1998). Because of the lower signal-to-noise ratio and broad peaks of satellite-altitude anomalies, the depths computed from $|A_n|$ at 400 km altitude have errors bars that are unacceptably large for geologic interpretation.

1.2. The idealized model study

An anomaly and its first and second vertical derivatives [$n=0$, 1, 2, respectively, Eq. (1)] were computed from an inductively magnetized prismatic model (25°E-35°E, 25°N-35°N in horizontal

dimensions, and 0–40 km in depth) using a spherical three-dimensional modeling method (von Frese et al., 1981). With respect to the observation elevation (400 km), the source is thin and, hence, it approximates a sill-like geologic body. Examples of the analytic signals from the anomaly and the first vertical derivative are shown in Fig. 1 for a midlatitudes situation (the geographic coordinates are for reference only and the coordinates or the other model parameters of the prismatic model source have no significance since the method is not affected by the varying geomagnetic field direction or the presence of remanence). The analytic signal of the second vertical derivative is noisy and not shown (the noise is caused by truncating the numerical representation to a few decimal digits as for the observed anomalies, henceforth called the "numerical truncation noise"). It is, however, known to yield good results with high-resolution aeromagnetic data (Hsu et al., 1998) and may be usable with a few lower satellite-altitude anomalies having higher signal-to-noise ratio (e.g. the Mars magnetic anomalies, Acuña et al., 1999). In both cases (Fig. 1), the maxima of the analytic signal are situated over the north and south edges of the source. The oval of the maxima narrows over the source edges for the first vertical derivative, indicating increased resolution with the derivative. The total intensity anomaly, on the other hand, exhibits the usual dipole pattern asymmetric with respect to the source (the total intensity anomaly is plotted in the figures associated with the Euler method part of the study, see Fig. 4). Relative maxima also occur near the eastern and western edges of the prism. The maxima on the east and west also sharpen with the increasing order of the derivative (Fig. 1a vs. Fig. 1b); however, they do not exactly overlie the edges. None of the published depth estimators based on the method (Roest et al., 1992; Hsu et al., 1996, 1998) had adequate resolution to yield the correct depths to these sources.

1.3. The analytic signal method applied to the Bangui anomaly

Fig. 2a and b shows the analytic signal of the total intensity magnetic anomaly computed from the model of Girdler et al. (1992) and the observed Magsat anomaly data [from the spherical harmonic model of Cain et al. (1990), ranging in degrees from 14 to 49], respectively. Fig. 3a and b illustrates the same for the first vertical derivative of the anomaly (instead of the total intensity magnetic anomaly). The analytic signal of the second vertical derivative of the observed anomaly is dominated by noise as in the theoretical case. Girdler et al. (1992) worked with an initial estimate of the anomaly field in this region. The Cain et al. (1990) anomaly field, which is shown to be one of the best representations of the anomaly field based on comparisons with the long aeromagnetic surveys in Canada by Ravat et al. (1998), is different in detail than the anomaly of (Girdler et al. 1992) and, hence, we will focus the comparison on the overall pattern of the analytic signal rather than the relative amplitudes of the analytic signal. For this disc-like source, from the satellite altitude, the maxima of the analytic signal overlie the entire source and not its edges: the circular outline and the relatively smaller dimensions of this source are the cause of the differences in the results with respect to the previous prismatic source case. However, the similarity of the pattern of the analytic signal of the model anomaly (Figs. 2a and 3a) and the observed data (Figs. 2b and 3b) is consistent with the idea of the impact related magnetization proposed by Girdler et al. (1992) for the primary source of the Magsat altitude Bangui anomaly. The evidence from the analytic signal is not conclusive; however, additional support for this model is provided by the results of the Euler method.

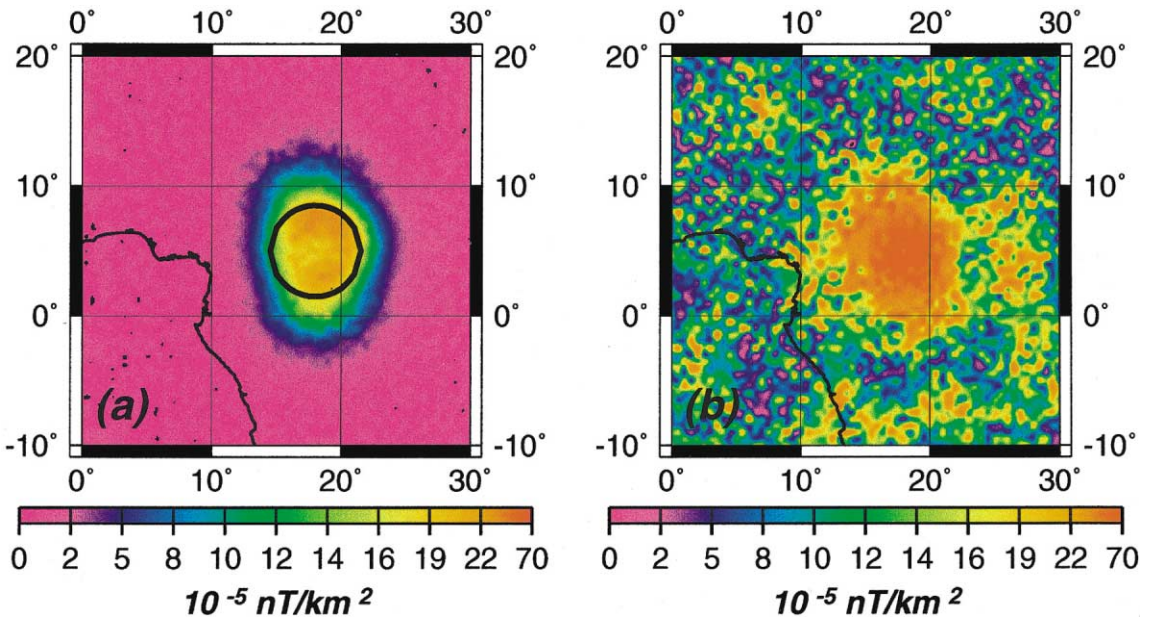

Fig. 3. The amplitude of the analytic signal of the first vertical derivative of the total intensity magnetic anomaly from (a) the impact model of Girdler et al. (1992) for the Bangui anomaly in central Africa, and (b) the anomaly field model of Cain et al. (1990) for the central African region. The heavy line shows the outline of the impact model. Observation elevation = 400 km. Grid spacing = 0.5°. See the caption of Fig. 1 for the details regarding the units and color scale.

2. The Euler method

In the Euler method, an estimate of the location of a source is derived from the anomalous field, its gradients, and the rate of the attenuation of the anomaly (which is based on the shape of the source). The method is applied in an overlapping moving window fashion and leads to a large number of solutions from which high quality solutions with the lowest numerical uncertainties (e.g. the top few per cent of all of the solutions) on the model parameters are selected (Thompson, 1982; Reid et al., 1990). The method suffers from a few drawbacks. It is best suited for sources for which the anomaly attenuation rate (N) is constant (for example, idealized magnetic sources such as spheres/dipoles ($N=3$), cylinders ($N=2$), edges of sills ($N=1$), etc.). For arbitrary sources, N changes from place to place, its magnitude is dependent on the size of the window, and there is a coupling (inter-dependency) between the N and the source-to-observation distance vector, which leads to errors in the depth estimate of the source (Ravat, 1996). The Euler method can also be used on the successive derivatives of the field to increase the resolution when high quality data are available.

The generalized Euler equation (Blakely, 1995) is

$$\vec{s} \cdot \vec{\nabla} T = -NT, \tag{2}$$

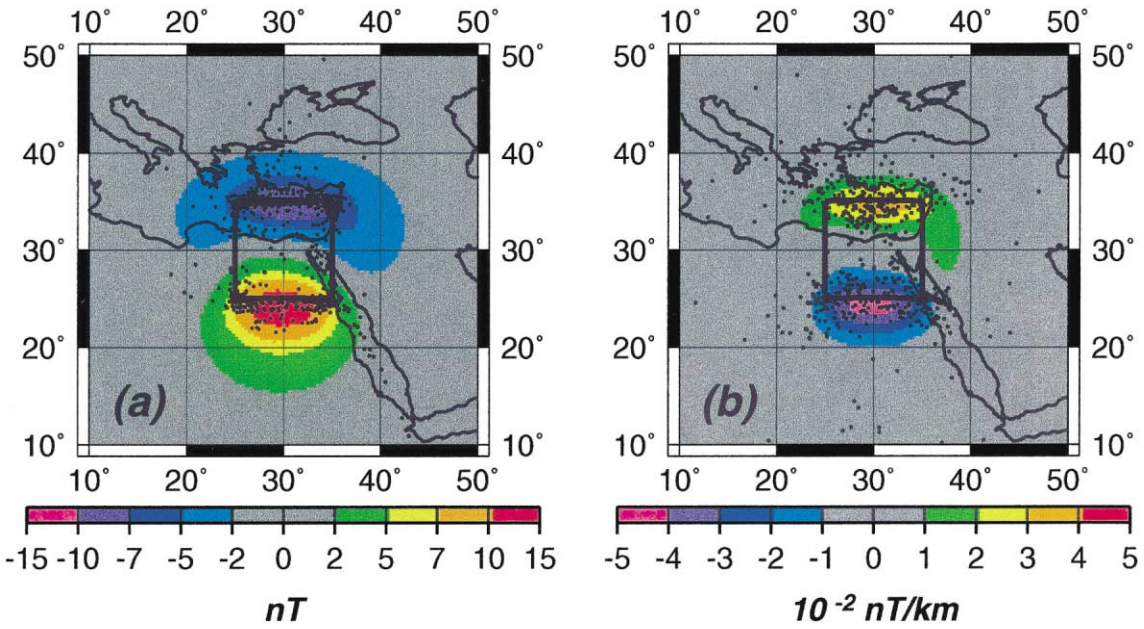

Fig. 4. The model study of the Euler method on (a) the total intensity magnetic anomaly ($n=0$) and (b) first vertical derivative ($n=1$) from a prismatic source. The selected Euler solutions are shown with black dots. Outline of the prismatic source is shown by the heavy lines. Window size = 3×3. $N=1$. Observation elevation = 400 km. Grid spacing = 0.5°.

where $\vec{s}$ is the source-to-observation distance vector, $\vec{\nabla}T$ is the gradient of the anomaly T, and N is the anomaly attenuation rate. Cast in the spherical coordinates appropriate for handling satellite data (factors $\frac{1}{r}$ and $\frac{1}{r\ \sin\theta}$ cancel) that considers higher order derivatives of the anomaly field, the generalized Euler equation becomes

$$(\theta-\theta_0)\ \frac{\partial}{\partial\theta}\left(\frac{\partial^n T}{\partial z^n}\right)+(\phi-\phi_0)\ \frac{\partial}{\partial\phi}\left(\frac{\partial^n T}{\partial z^n}\right)+(z-z_0)\ \frac{\partial}{\partial z}\left(\frac{\partial^n T}{\partial z^n}\right)\quad=\quad-(N+n)\left(\frac{\partial^n T}{\partial z^n}\right) \tag{3}$$

where T is the total intensity magnetic anomaly, n is the order of the derivative, θ, ϕ, z are the spherical coordinates of the observation location, θ_0, z_0, are the spherical coordinates of the source location, and N is the anomaly attenuation rate. The variable z is being used, instead of the usual spherical coordinate r, to indicate the downward direction of the coordinate in this problem. The notation $\frac{\partial^n T}{\partial_z^n}$ is the same as in Eq. (1).

2.1. The idealized model study

A model study was carried out on the previously described idealized prismatic source (shown in Fig. 1) using the total intensity anomaly and its radial derivatives. The Euler solutions (with $N=1$, designed to mark the edges of source) are situated over the north and south edges of this

source for both the total intensity and vertical derivative fields (Fig. 4a and b, respectively). It appears that the solutions are slightly more scattered for the vertical derivative field (Fig. 4b), indicating the effect of the numerical truncation noise (defined earlier). As shown later with the example of a circular disc, the effect of noise could be reduced by increasing the window size. The second derivative field did not yield useful results from this altitude. With larger prisms (not shown), there is a higher concentration of solutions near all of the edges and corners of the sources. In all of these cases, the depth estimates are spread roughly ±100 km about the true depth of the sources. Hence, the resolution of the method is not adequate to determine the depth to the top of the sources from these high elevations.

2.2. The Euler method applied to the Bangui anomaly

Fig. 5a and b shows the selected Euler solutions from the anomaly computed from the model of Girdler et al. (1992) and the observed Magsat anomaly field (Cain et al., 1990), respectively. In both cases, the solutions appear in a slightly elliptical pattern surrounding the edge of the interpreted impact ring. The solutions from the observed anomaly are stretched in the NE direction (instead of the EW direction for the idealized model) suggesting perhaps the geologic complexity introduced by other sources in the region or later localized remagnetizations. Furthermore, in the solutions from the observed data, there is a concentration near the center of the ring (5°N, 18°E) (Fig. 5b), indicating the presence of an additional highly magnetic source.

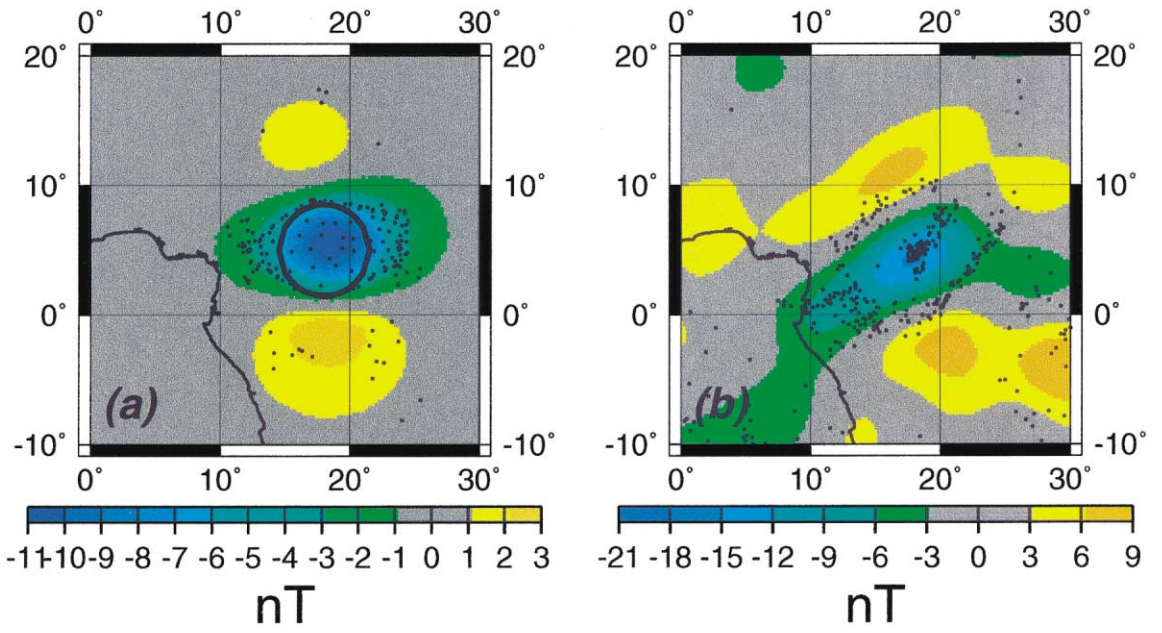

Fig. 5. Application of the Euler method on the total intensity magnetic anomaly (n = 0) from (a) the impact model of Girdler et al. (1992) for the Bangui anomaly in central Africa, and (b) the anomaly field model of Cain et al. (1990) for the central African region. The selected Euler solutions are shown with black dots. The heavy line shows outline of the impact model. Window size = 3×3. $N = 1$. Observation elevation = 400 km. Grid spacing = 0.5°.

We have also tested with this method another geologic forward model presented for the Bangui anomaly and the surrounding region [from Ravat et al. (1992), and also shown in Langel and Hinze (1998), which also takes into account aspects of the interpretation of Regan and Marsh (1982) and Hastings (1982)]. The solutions from that model (not shown here, but they very well outline the sources assumed in that model [see Fig. 7 in Ravat et al. (1992)] and the observed anomaly are quite different, except for the central highly concentrated magnetic source. Similarity of the pattern of the solutions from the impact model and the observed data indicate that the impact-related magnetization sources (the ring as well as the central highly magnetic source) are possible contributors to the anomaly.

Although the Euler solutions on the first vertical derivative of the observed anomaly field did not yield usable results due perhaps to noise in the observed data, we have presented here the derivative results from the impact model (Fig. 6). These results are computed with a larger window size to reduce the effect of the numerical truncation noise in the computation of derivatives. The solutions clearly define the circular ring pattern near the edges of the model source illustrating the possibilities this method has with high quality and low altitude satellite data. For the case of the vertical derivative, with the larger window, a small concentration of solutions appears near the center of the source. However, we do not think that the central zone of solutions for the Bangui anomaly itself (Fig. 5b) is an artifact because we were not able to simulate this from the model study of the total intensity data. Moreover, unlike Fig. 6, the central area of the Bangui anomaly has a very large number of solutions. Furthermore, Project Magnet and ground magnetic data shown by Green (1976) and Regan and Marsh (1982) show also isolated 800–1000 nT

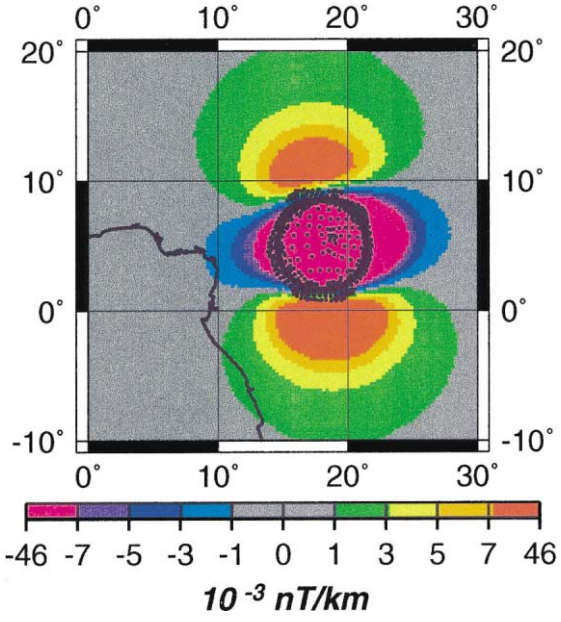

Fig. 6. The model study of the Euler method on the first vertical derivative ($n=1$) of the magnetic anomaly from the impact model of Girdler et al. (1992) for the Bangui anomaly in central Africa. The selected Euler solutions are shown with black dots. Window size = 10×10. $N=1$. Observation elevation = 400 km. Grid spacing = 0.5°.

anomalies of 100–200 km wavelength embedded within broader magnetic anomalies associated with the Bangui anomaly. Thus, it is certain that a number of highly concentrated magnetic sources exist within this central region.

3. Discussion and conclusion

Using model studies on idealized sources and examples from the observed Magsat data, we have demonstrated the utility of the gradient-based Euler and analytic signal methods in the interpretation of satellite-altitude magnetic data. The results of the analytic signal of the Bangui magnetic anomaly in central Africa and its vertical derivative and the model based on the impact hypothesis are similar in appearance, supporting the interpretation that the anomaly is partly caused by magnetization associated with a large meteoritic impact (Girdler et al., 1992). Euler solutions from the anomaly (Fig. 5b) provide an elliptical outline in the vicinity of the hypothesized impact zone, the location of which is based on independent topographic data. The Euler solutions from the anomaly computed from a circular disc-like model source (Fig. 5a) also yield a similar distribution of the solutions, giving additional credibility to the impact hypothesis. As additional support, inversion results without assuming purely induced magnetization (Whaler and Langel, 1996) are also in agreement with a partly remanently magnetic source for the Bangui anomaly (Langel and Hinze, 1998). The Euler solutions further indicate another highly magnetic source in the vicinity, similar to the concentrated source modeled by Ravat (1989) and Ravat et al. (1992) in central Africa, suggesting that parts of this possible large iron-bearing meteorite may still be buried near the central part of the ring structure (Green, 1976). This interpretation, although speculative, has important economic implications.

Although the possibility of an ancient age for the impact is suggested (Girdler et al., 1992), the age is uncertain. Neither the higher impact population early in the history of the terrestrial bodies (Grieve, 1987) nor the small mean impact interval for the larger size impacts on the Earth (Table 2.1 in French, 1998) preclude large impacts from occurring later in the Earth's history. Certainly, radiogenic lead isotopic composition of carbonados in the region gives an estimated age between 2.6 and 3.8 Ga (Ozima and Tatsumoto, 1997) and favors the impact hypothesis. A meteoritic impact is one of the many hypotheses for the origin of carbonados (Smith and Dawson, 1985; Ozima and Tatsumoto, 1997; Haggerty, 1999).

In the impact model, the impactor energy would be sufficient to melt a portion of the target rock (Grieve, 1987). Generally the impact melt is confined to the crater basin and therefore would take a generally circular shape. In the Girdler et al. (1992) report, the circular outline depicted by the East-gradient of the topography was presented, together with the large magnetic anomaly, as a possible representation of the original impact. Opposing arguments, however, suggested that subsequent tectonic deformation and erosion would obliterate any surface expression produced by an ancient impact event. In the counter argument, it should be pointed out that the present topographic expression of a circular shape would, most likely, be the exhumed scar of the hardened rim of the original event. Furthermore, it is well established that impact craters on Earth have associated magnetic anomalies (e.g. Pilkington and Grieve, 1992; also the large dimension Chicxulub Crater, Rebolledo-Vieyra et al., 2000). In this model, we might assume that the remanent magnetization would be a thermal remanent magnetization (TRM). Significant

hydrothermal activity is also associated with an impact event (see, for example, Melosh, 1989, Sections 5.2 and 8.2) and we cannot, therefore, rule out chemical remanent magnetization as well. In addition, perhaps shock remanent magnetization may play a small role (see, for example, Srnka et al., 1979, or Cisowski and Fuller, 1978). Most likely the remanent magnetization of the Bangui anomaly is a complex combination of some or all of the above.

Finally, the theoretical examples presented in the paper show that the gradient methods would be important in analyzing high quality magnetic data from the Oersted and CHAMP satellites and interpreting the extremely large remanently magnetic anomalies observed by the Mars Global Surveyor spacecraft. The methods discussed in the paper would also benefit from direct observations of the gradients of the field from a low altitude magnetic gradiometer mission.

Acknowledgements

D.R. developed the methods in this paper primarily to disprove the circular disc model of Girdler et al. (1992). However, the objective evidence of the source edges from the Euler method from the Bangui anomaly, roughly in the form of a disc, made him retract his long-standing opposition. We are especially grateful to James J. Frawley and Professor Ronald W. Girdler for numerous discussions related to these interpretations. We thank Prof. Kathy Whaler for a number of improvements. We also thank three anonymous reviewers for their helpful comments on the paper and the editor Dr. Eigil Friis-Christensen for facilitating the review process. The research was conducted through the funding provided by NASA. We are grateful for this support.

References

Acuña, M., Connerney, J., Ness, N., Lin, R., Mitchell, D., Carlson, C., McFadden, J., Anderson, K., Rème, H., Mazelle, C., Vignes, D., Wasilewski, P., Cloutier, P., 1999. Global distribution of crustal magnetization discovered by the Mars Global Surveyor MAG/ER experiment. Science 284, 790–793.

Blakely, R.J., 1995. Potential Theory in Gravity and Magnetic Applications. Cambridge University Press, Cambridge, 441p.

Cain, J.C., Holter, B., Sandee, D., 1990. Numerical experiments in geomagnetic modeling. J. Geomag. Geoelectr. 42, 973–987.

Cisowski, S.M., Fuller, M., 1978. The effect of shock on the magnetism of terrestrial rocks. J. Geophys. Res. 83, 3441–3458.

French, B.M., 1998. Traces of Catastrophe: A Handbook of Shock-Metamorphic Effects in Terrestrial Meteorite Impact Structures. LPI contribution no. 954. Lunar and Planetary Institute, Houston. 120pp.

Girdler, R.W., Taylor, P.T., Frawley, J.J., 1992. A possible impact origin for the Bangui magnetic anomaly (Central Africa). Tectonophysics 212, 45–58.

Green, A.G., 1976. Interpretation of project MAGNET aeromagnetic profiles across Africa. Geophys. J. R. Astron. Soc. 44, 203–228.

Grieve, R.A.F., 1987. Terrestrial impact structures. Ann. Rev. Earth Planet. Sci. 15, 245–270.

Haggerty, S.E., 1999. A diamond trilogy: superplumes, supercontinents, and supernovae. Science 285, 851–860.

Hastings, D.A., 1982. Preliminary correlations of MAGSAT anomalies with tectonic features of Africa. Geophys.Res.Lett. 9, 303–306.

Hsu, S.-K., Coppens, D., Shyu, C.-T., 1998. Depth to magnetic source using the generalized analytic signal. Geophysics 63, 1947–1957.

Hsu, S.-K., Sibuet, J.-C., Shyu, C.-T., 1996. High-resolution detection of geologic boundaries from potential-field anomalies: an enhanced analytic signal technique. Geophysics 61, 373–386.

Langel, R.A., Hinze, W.J., 1998. The Magnetic Field of the Earth's Lithosphere: The Satellite Perspective. Cambridge University Press, Cambridge. 429p.

Melosh, H.J., 1989. Impact Cratering: A Geologic Process, Oxford Monographs on Geology and Geophysics: No. 11. Oxford University Press, Oxford. 245p.

Nabighian, M.N., 1972. The analytic signal of two-dimensional magnetic bodies with polygonal cross section: its properties and use for automated anomaly interpretation. Geophysics 37, 507–517.

Nabighian, M.N., 1974. Additional comments on the analytic signal of two-dimensional magnetic bodies with polygonal cross section. Geophysics 39, 85–92.

Ozima, M., Tatsumoto, M., 1997. Radiation induced diamond crystallization: Origin of carbonados and its implications on meteorite nano-diamonds. Geochimica et Cosmochimica Acta 61, 369–376.

Pilkington, M., Grieve, R., 1992. The geophysical signature of terrestrial impact craters. Rev. Geophys. 30, 161–181.

Ravat, D., 1989. Magsat Investigations over the Greater African Region, PhD dissertation, Purdue University, West Lafayette, 234p.

Ravat, D., 1996. Analysis of the Euler method and its applicability in environmental magnetic investigations. J. Env. Eng. Geophys. 1, 229–238.

Ravat, D., Hinze, W.J., von Frese, R.R.B., 1992. Analysis of Magsat magnetic contrasts across Africa and South America. Tectonophysics 212, 59–76.

Ravat, D., Pilkington, M., Purucker, M., Sabaka, T., Taylor, P.T., von Frese, R.R.B., Whaler, K.A., 1998, Recent advances in the verification and geologic interpretation of satellite-altitude magnetic anomalies. In: 68th Ann. Meeting, Soc. Expl. Geophysicists, Expanded abstracts, pp. 507–510.

Rebolledo-Vieyra, M., Vera-Sanchez, P., Urrutia-Fucugauchi, J., Soler-Arechalde, A.M., 2000. Modeling of aeromagnetic anomalies of the Chicxulub Crater and its implications on the nature of the Yucatan basement. EOS Trans. Am. Geophys. Un. 81 (48), F802.

Regan, R.D., Marsh, B.D., 1982. The Bangui magnetic anomaly: its geologic origin. J. Geophys. Res. 87, 1107–1120.

Regan, R.D., Cain, J.C., Davis, W.M., 1975. A global magnetic anomaly map. J. Geophys. Res. 80, 794–802.

Reid, A.B., Allsop, J.M., Granser, H., Millett, A.J., Somerton, I.W., 1990. Magnetic interpretation in the three dimensions using Euler deconvolution. Geophysics 55, 80–91.

Roest, W.R., Verhoef, J., Pilkington, M., 1992. Magnetic interpretation using the 3-D analytic signal. Geophysics 57, 116–125.

Smith, V.J., Dawson, J.B., 1985. Carbonados: diamond aggregates from early impacts of crustal rocks? Geology 13, 342–343.

Srnka, L.J., Martelli, G., Newton, G., Cisowski, S.M., Fuller, M.D., Schaal, R.B., 1979. Magnetic field and shock effects and remanent magnetization in a hypervelocity experiment. Earth Planet. Sci. Letters 42, 127–137.

Thompson, D.T., 1982. EULDPH: a new technique for making computer-assisted depth estimates from magnetic data. Geophysics 47, 31–37.

von Frese, R.R.B., Hinze, W.J., Braile, L.W., Luca, A.J., 1981. Spherical earth gravity and magnetic anomaly modeling by Gauss-Legendre quadrature integration. J.Geophys. 49, 234–242.

Whaler, K.A., Langel, R.A., 1996. Minimal crustal magnetizations from satellite data. Phys. Earth Planet. Int. 98, 303–314.